



A Comprehensive Evaluation Of The Effect Of Various Strength Parameters In Ferrous Material With Variation In Percentage Of Carbon

¹Munish Baboria , ²Harsimran Singh

¹Assistant Professor, ²Assistant Professor

¹Department of Mechanical Engineering,

¹Government College of Engineering and Technology, Chak Bhalwal, Jammu

²Department of Mechanical Engineering,

¹Government College of Engineering and Technology, Chak Bhalwal, Jammu

Abstract: Iron stands as the cornerstone of numerous industrial applications, with steels and iron alloys holding a dominant position in the manufacturing sector worldwide owing to its remarkable properties like high tensile strength, excellent corrosion resistance, and easy machinability. The continual exploration and utilization of iron in innovative ways underscore its enduring importance in shaping the modern world and beyond. These properties can be significantly altered by varying the carbon percentage in iron to create different types of steel. By understanding the effects of carbon content on the properties of virgin iron, engineers and manufacturers can tailor steel grades to meet specific performance requirements in various industries, ensuring optimal results in diverse applications. In this paper, effect of carbon contents variations on properties like hardness, elongation, tensile as well as yield strength is analysed using hardness testing machine and Universal Testing Machine (UTM) and optical Spectrometer. The results so obtained are at par with available literature and hence, validates the research work.

Index Terms : Carbon, elongation, iron, iron carbon diagram, hardness, spectrometer, steel, tensile strength and yield stress.

I. INTRODUCTION

Iron is a vital element denoted by the chemical symbol **Fe**, derived from the Latin word "ferrum," holding an atomic number of 26. Situated in the initial transition series of metals, it stands as the prevailing constituent by mass-shaping the entire planet Earth, contributing significantly to both the inner and outer core. Occupying the fourth position in terms of ubiquity in the Earth's crust, iron's omnipresence in terrestrial bodies like Earth can be attributed to its prolific generation through fusion in massive stars. The aftermath of the fusion process results in the production of nickel-56, eventually decaying into the most prevalent isotope of iron. This cascades into the formation of iron in significant quantities before the culmination of a supernova event disperses this precursor radionuclide extensively into space. Operating within a broad spectrum of oxidation states, ranging from -2 to +6, although the states +2 and +3 are the most prevalent. While raw iron can be found in meteoroids and low-oxygen environments, it undergoes rapid reactions in the presence of oxygen and water. Initially presenting as a shiny silvery-gray surface, it eventually undergoes oxidation in regular air, giving way to the formation of hydrated iron oxides, commonly referred to as rust. Unlike various other metals that develop protective oxide layers, iron oxides consume more space than iron metal, causing them to flake off and unveil fresh surfaces, thereby accelerating the corrosion process. Dating back to ancient civilizations, the utilization of iron has been prevalent; however, the preference for copper alloys with lower melting temperatures was prominent initially. While pure iron is relatively soft, impurities introduced during the

smelting process, particularly carbon, significantly enhance its hardness and strength. An optimal proportion of carbon, ranging between 0.2% and 2.1%, yields steel, boasting hardness levels up to a thousand times greater than pure iron. The production of crude iron metal takes place in blast furnaces, where ore is reduced using coke to yield pig iron characterized by a high carbon content. Subsequent refinement with oxygen diminishes the carbon content to the required level for producing steel. Widely utilized across industries, steels and iron alloys blended with other metals (alloy steels) stand as the predominant metals, renowned for their diverse and desirable properties worldwide. Continuing the discussion on iron, it's fascinating to delve into its prevalence and significance not just on Earth, but throughout the Universe. Iron, being the sixth most abundant element in the cosmos and the most common refractory element, plays a critical role in stellar nucleosynthesis. Formed as a result of the final exothermic phase of silicon fusion in massive stars, iron's abundance is a testament to its crucial role in the cosmic processes that shape our universe. While metallic or native iron is seldom found on Earth's surface due to its inherent susceptibility to oxidation, its oxides are pervasive and represent the primary ores from which we extract this essential metal. The Earth's inner and outer core are believed to principally comprise an iron-nickel alloy, accounting for a substantial portion of the planet's overall mass.

1.2 Occurrence

Iron is the sixth most abundant element in the universe and the most common refractory element. It is formed as the final exothermic stage of stellar nucleon synthesis, by silicon fusion in massive stars. Metallic or native iron is rarely found on the surface of the Earth because it tends to oxidize, but its oxides are pervasive and represent the primary ores. While it makes up about 5% of the Earth's crust, both the Earth's inner and outer core are believed to consist largely of an iron-nickel alloy constituting 35% of the mass of the Earth as a whole. Iron is consequently the most abundant element on Earth, but only the fourth most abundant element in the Earth's crust. Iron meteorites are of similar composition of earth's inner and outer core. Most of the iron in Earth's rocks combines with oxygen to form iron oxide minerals such as hematite and magnetite. Large iron ore deposits are found in banded iron ore layers consisting of trailing thin layers of iron oxide (magnetite (Fe_3O_4) or hematite (Fe_2O_3)).

1.3 Classification

The addition of carbon to iron forms the metal called steel. By controlling the amount of carbon added to steel, different types of steel with different properties can be produced. Carbon monoxide is an important element in steel production because it affects the strength, hardness, and other properties of metal alloys. Steel with more carbon will be harder, stronger but brittle, while steel with lower content will be softer and ductile. Specific properties of steel can be changed by adjusting the carbon content during production. The amount of carbon added to the metal affects the properties of the resulting metal. These carbon contents in iron lead to its classification into the following types:

1.3.1 Cast Iron

Ferrous metals are those that contain iron as the base metal. The properties of ferrous metals may be changed by adding cast iron is a metal that is widely used. It is hard, brittle, and has good wear resistance. Cast iron contains 2 to 4 percent carbon that need to be combined to produce a metal to serve a percent carbon. White cast iron is very hard and is used for specific purposes. The source of ferrous metal is pig iron. Pig iron is used only for the required wear resistance and abrasion resistance. White metal is produced in a blast furnace containing cast iron heated to render the metal unusable; The four types of iron ore are hematite, limonite, magnetite, and ferrite. Malleable cast iron is stronger and harder than white cast iron; however, it is more expensive to make. Gray cast iron is another type of cast iron. It is often used in castings because it can easily flow into complex shapes.

1.3.2 Steel

Steel is an alloy of iron and carbon or other alloying elements. When the alloying element is carbon, the steel is referred to as carbon steel. Carbon steels are reclassified by the percentage of carbon in "points" or hundredths of 1 percent they contain.

1.3.3 Low Carbon Steel

It contains carbon content up to 0.30 percent or 30 points. This steel is soft and ductile and can be rolled, punched, sheared, and worked when either hot or cold. It is easily machined and can be readily welded by all methods. It does not harden to any great amount; however, it can be easily case or surface-hardened

1.3.4 Medium Carbon Steel

It contains carbon content from 0.30 to 0.50 percent or 30 to 50 points, this steel may be heat-treated after fabrication. It is used for general machining and forging of parts that require surface hardness and

strength. It is made in bar form in the cold-rolled or normalized and annealed condition. During welding, the weld zone will become hardened if cooled rapidly and must be stress-relieved after welding.

1.3.5 High Carbon Steel

It contains carbon content from 0.50 to 1.05% or 50 to 105 points. This steel is used in the manufacture of drills, taps, dies, springs, and other machine tools and hand tools that are heat treated after fabrication to develop the hard structure necessary to withstand high shear stress and wear. It is manufactured in bar, sheet, and wire forms, and in the annealed or normalized condition to be suitable for machining before heat treatment. This steel is difficult to weld because of the hardening effect of heat at the welding joint.

1.3.6 Tool Steel.

It contains carbon content from 0.90 to 1.70 percent or 90 to 170 points. This steel is used in the manufacture of chisels, shear blades, cutters, large taps, woodturning tools, blacksmith's tools, razors, and other similar parts where high hardness is required to maintain a sharp cutting edge. It is difficult to weld due to the high carbon content.

1.3.7 High-Speed Steel

High-speed steel is a self-hardening steel alloy that can withstand high temperatures without becoming soft. High-speed steel is ideal for cutting tools because of its ability to take deeper cuts at higher speeds than tools made from carbon steel.

1.3.8 Alloy Steels

Steel is manufactured to meet a wide variety of specifications for hardness, toughness, machineability, and so forth. Manufacturers use various alloying elements to obtain these characteristics, when elements other than carbon, such as chromium, manganese, molybdenum, nickel, tungsten, and vanadium are used. The resulting metals are called alloy steels show some of the general characteristics obtained by the use of various alloying elements.

1.4 Iron Carbon Equilibrium Diagram

Iron-carbon (Fe-C) phase diagram is a graphical representation of the phases and phase transitions that occur in iron-carbon alloys as a function of temperature and carbon content. The iron-carbon diagram typically shows the different phases of iron (ferrite, austenite, cementite, and others) and how they change with varying carbon content and temperature. The main phases that are commonly represented in the diagram are:

1. Austenite (γ): This is a face-centered cubic (FCC) phase of iron that exists at high temperatures.
2. Ferrite (α): This is a body-centered cubic (BCC) phase of iron that exists at lower temperatures.
3. Cementite (Fe_3C): This is an intermetallic compound of iron and carbon that is very hard and brittle.

The iron-carbon phase diagram is a vital tool in the field of metallurgy for understanding the relationship between the composition, microstructure, and properties of iron-carbon alloys. By manipulating the cooling rate and carbon content during the solidification process, different microstructures can be obtained, leading to a wide range of mechanical properties in steels. One critical aspect of the iron-carbon diagram is the concept of phase transformations. For example, when a steel alloy is slowly cooled from a high temperature, the austenite phase can transform into different microstructures like pearlite, bainite, or martensite, depending on the cooling rate and composition. These different microstructures have a significant impact on the hardness, strength, toughness, and other mechanical properties of the material. It should first be pointed out that the normal equilibrium diagram really represents the metastable equilibrium between iron and iron carbide (cementite). Cementite is metastable and the true equilibrium should be between iron and graphite. Although graphite occurs extensively in cast irons (2-4 wt % C), it is usually difficult to obtain this equilibrium phase in steel (0.03-1.5 wt % C). Therefore, the metastable equilibrium between iron and iron carbide should be considered, because it is relevant to the behaviour of most steels in practice. The much larger phase field of γ -iron (austenite) compared with that of α -iron (ferrite) reflects the much greater solubility of carbon in γ -iron, with a maximum value of just over 2 wt % at 1147°C denoted by E in **Figure 1**

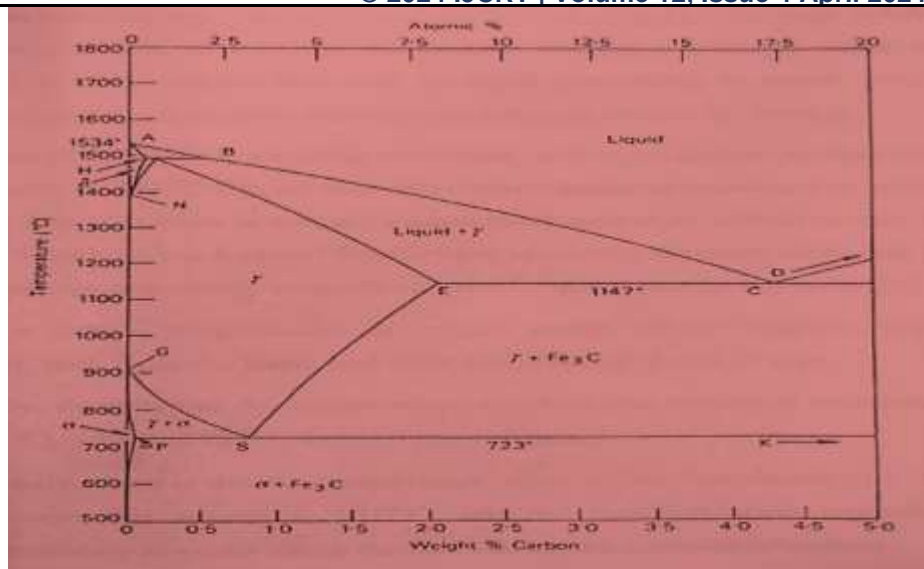


Figure 1. Iron-Carbon diagram

This high solubility of carbon in γ -iron is of extreme importance in heat treatment, when solution treatment in the γ -region followed by rapid quenching to room temperature allows a supersaturated solid solution of carbon in iron to be formed. The α -iron phase field is severely restricted, with a maximum carbon solubility of 0.02 wt% at 723°C (P), so over the carbon range encountered in steels from 0.05 to 1.5 wt%, α -iron is normally associated with iron carbide in one form or another. Similarly, the γ & δ -phase field is very restricted between 1390 and 1534°C and disappears completely when the carbon content reaches 0.5 wt% (B). There are several temperatures or critical points in the diagram, that are important, both from the basic and from the practical point of view.

Firstly, there is the A_1 temperature at which the eutectoid reaction occurs (P-S-K), which is 723°C in the binary diagram.

Secondly, there is the A_2 , temperature when α -iron transforms to γ -iron. For pure iron this occurs at 910°C, but the transformation temperature is progressively lowered along the line GS by the addition of carbon. The third point is A_3 , at which γ -iron transforms to δ -iron, 1390°C in pure iron, but this is raised as carbon is added. The A_2 point is the Curie point. when iron changes from the ferro to the paramagnetic condition. This temperature is 769°C for pure iron, but no change in crystal structure is involved. The A_1 , A_2 and A_3 points are easily detected by thermal analysis or dilatometry during cooling or heating cycles, and some hysteresis is observed.

Consequently, three values for each point can be obtained. A_c for heating, A_r for cooling and A_e (equilibrium), but it should be emphasized that the A_c and A_r values will be sensitive to the rates of heating and cooling, as well as to the presence of alloying elements. The great difference in carbon solubility between γ - and α -iron leads normally to the rejection of carbon as iron carbide at the boundaries of the γ phase field. The transformation of γ to α iron occurs via a eutectoid reaction, which plays a dominant role in heat treatment. The eutectoid temperature is 723°C while the eutectoid composition is 0.80% C. On cooling alloys containing less than 0.80% C slowly, hypo-eutectoid ferrite is formed from austenite in the range 910-723°C with enrichment of the residual austenite in carbon, until at 723°C the remaining austenite, now containing 0.8% carbon transforms to pearlite, a lamellar mixture of ferrite and iron carbide (cementite). In austenite with 0.80 to 2.06% carbon, on cooling slowly in the temperature interval 1147°C to 723°C, cementite first forms progressively depleting the austenite in carbon, until at 723°C, the austenite contains 0.8% carbon and transforms to pearlite. Steels with less than about 0.8% carbon are thus hypo-eutectoid alloys with ferrite and pearlite as the prime constituents, the relative volume fractions being determined by the lever rule which states that as the carbon content is increased, the volume percentage of pearlite increases, until it is 100% at the eutectoid composition. Above 0.8% C, cementite becomes the hyper-eutectoid phase, and a similar variation in volume fraction of cementite and pearlite occurs on this side of the eutectoid composition. The three phases, ferrite, cementite and pearlite are thus the principal constituents of the infrastructure of plain carbon steels, provided they have been subjected to relatively slow cooling rates to avoid the formation of metastable phases.

1.4.1 The austenite- ferrite transformation

As a rule, subangular ferrite will form in iron-carbon alloys containing up to 0.8% carbon. This reaction occurs in pure iron at 910°C, but in iron-carbon alloys it occurs between 910°C and 723°C. However, ferrite can be formed from its austenite state by quenching to temperatures as low as 600°C. As below the eutectoid temperature. As the transition temperature decreases, a clear transition occurs and it should be said that this transition applies mainly to the sub-eutectoid and supra-eutectoid phases, although in each case there will be changes depending on the actual crystallography of the affected phases. For example, the same principle applies to austenite forming cementite, but morphologically it is not easy to distinguish between ferrite and cementite.

1.4.2 The austenite-cementite transformation

The Dube classification applies equally well to the various morphologies of cementite formed at progressively lower transformation temperatures. The initial development of grain boundary allotriomorphs is very similar to that of ferrite and the growth of side plates or Widmanstätten cementite follows the same pattern. The cementite plates are more rigorously crystallographic in form, despite the fact that the orientation relationship with austenite is a more complex one. As in the case of ferrite, most of the side plates originate from grain boundary allotriomorphs, but in the cementite reaction more side plates nucleate at twin boundaries in austenite.

1.4.3 The austenite-pearlite reaction

Pearlite is probably the most familiar micro structural feature in the whole science of metallography. It was discovered by Sorby over 100 years ago, who correctly assumed it to be a lamellar mixture of iron and iron carbide. Pearlite is a very common constituent of a wide variety of steels, where it provides a substantial contribution to strength. Lamellar eutectoid structures of this type are widespread in metallurgy, and frequently pearlite is used as a generic term to describe these structures.

II. LITERATURE REVIEW

Carbon alloyed steel is broadly used in many manufacturing procedures keeping in view, its versatile mechanical properties, which strongly depend on carbon content material and manufacturing manner. Usually, the higher carbon content consequences in better tensile homes, with much less ductility and fabrication issues. As a carbon metallic is slowly cooled, primary ferrite (hypereutectoid steel) or number one cementite (hypereutectoid metal) begins to nucleate at austenite grain obstacles till below eutectoid temperature, the rest austenite decomposes into a lamellar structure of solid stages, by using the cooperative growth of cementite (Fe_3C) and ferrite at a commonplace transformation the front with the determine austenite by a eutectoid response [2]. Although the microstructure becomes lamellar or fully pearlitic as carbon content processes 0.8 wt.%C. The precipitation of small cementite debris was reported by [3] and has been verified in unalloyed steels containing variable carbon contents (in percentage) through using thermal treatment. The addition of alloying factors can adjust the section transformation situations in steels. It is pertinent to mention that all alloying elements retard pearlite transformation kinetics excluding cobalt (Co) [4]. Numerous works have been finished approximately the kinetics of pearlite transformation caused by alloying layout [5-8]. Bain [5] proposed the discount of proeutectoid ferrite fraction due to the fact manganese (Mn) changed the location of the vital factor of steels to decrease temperature and decrease carbon regions. While [6] determined that the chromium (Cr) and molybdenum (Mo) addition increased the eutectoid temperature, which promoted the high power of pearlite due to the refinement of the interlamellar spacing. Furthermore, it has been pronounced that the silicon (Si) addition ought to suppress the spheroidization of the cementite lamellae [7]. Previous work reported that the addition of ≥ 1 wt.% Ni could promote bainitic transformation at the fee of pro eutectoid ferrite in the Fe-Cr-Mo-C sintered steels [8]. The work of [2] claimed that once the isothermal heat remedy turned into hired, the divorced eutectoid transformation (DET) product changed into simply shown as spheroidal cementite debris in a ferrite matrix. DET came about through a non-cooperative increase mode resulting from the discern austenitic section consisting of cementite particles with some microns of spacing DET passed off due to the incorporation of partitioned carbon into the existing cementite debris. The theory proposed by [9] pronounced that with the aid of using a gradual cooling fee, the microstructure of excessive-carbon steel alloyed with molybdenum consisted of coarse degenerated pearlite, nanometer- sized molybdenum carbides and ferrite. Higher and decrease bainite structures also fashioned by way of non-cooperative eutectoid alterations [10]. The research work of [11] discovered that very best cementite debris were sincerely observed in excessive- carbon steels round 1.5 wt.%. The transformation the front, having a

mobile-shaped austenite/ferrite boundary, superior into an array of austenite plus fine cementite particles in a ferrite matrix. It has been said by [12] that pearlite with lamellae of ferrite and Mn_3C_6 carbide instead of Mn_3C plate has been determined in Fe-C-Cr alloys. The partitioning of Mn, Al, and C solutes changed into genuinely determined in the Mn_3C_6 pearlite of the FeC-Mn-Al alloy [13]. Numerous research were pronounced that softening procedures, of bearing steels, to create very last shape as coarse cementite particles dispersed in a matrix of ferrite [14,15,16]. It also referred to as a divorced pearlite, since the product phases no longer grew cooperatively. Furthermore, [17] observed that addition of Cr is best in minimizing carbide size. Due to the fact the morphology and dispersity of cementite and alloy carbide are important for the energy and ductility of alloyed steels therefore the stability among the carbon content and other alloying so that it will manipulate phase transformation, is the key to achieve excessive overall performance sintered metallic. Mo with quantities of 0.5-1.0 wt.%, is generally utilized in high power steels. It has excessive affinity for C and tendencies to transform into carbides throughout sintering. Further, Mo additionally walls to different carbides and bureaucracy its very own collection of carbides [18]. Though, there are some researches work approximately the effect of excessive-degree carbon addition on section transformation behaviours in quaternary alloy sintered metallic. The microstructures of sintered alloys containing carbon contents inside the range of 0.30-0.75 wt.% (with increment of 0.15%) changed in keeping with carbon content. The microstructures had twin-section structures, which composed of pf grains and zones of non-cooperative eutectoid decomposition products. The latter zones contained particles with distinct sizes and morphologies, which trusted the degree of undercooling, embedded in a gentle ferritic matrix. The non-cooperative eutectoid decomposition merchandise shaped in those sintered alloys are attributed especially to the effects of alloying Mo and Mn elements, that could retard the formation of pearlite [19]. Except, the fraction of those products also will increase with growing carbon content. The formation of the eutectoid transformation product happened underneath situations that low undercooling and small inter-particle spacing or high-quality array of pre-current cementite due to the advancing transformation the front begins to pull-away from cementite [20, 21]. Austenite and pearlite coexist in equilibrium have been supplied inside the three-segment areas, austenite (γ) + ferrite (α) + cementite (θ) of Fe-Fe₃C section diagram because of Mo and Mn moved the eutectoid temperature and also changed the eutectoid composition to lower carbon content material [2]. It could be defined that the transformation started out by way of proeutectoid carbide precipitation at grain boundary. After that, the austenite converted by eutectoid response into mixtures of non-cooperative and cooperative of ferrite and carbide. With increasing undercooling and carbon content, the transformation merchandise became smaller and more densely dispersed. The transformation collection can be explained through partitioning of the substitutional and interstitial element c coupled with a trade within the mechanism of transformation with undercooling [22]. According to the paintings carried out via the use of thermomechanical processing on the two steels with 0.46% C and 0.76% C, finer pearlite interlamellar spacing and spheroidized pearlite showed increase of energy without lack of durability and ductility [23]. Therefore, the present work aims to investigate the effect of medium-to-high-carbon contents on the final microstructures and mechanical properties of ferrous specimens.

III. EXPERIMENTAL SET UP AND METHODOLOGY

The research work is based on the estimation of variation in strength and elongation of ferrous specimens with the addition of carbon content in them. These properties are to be estimated using hardness testing machines. The properties to be analyzed in this research work can be summarized as:

3.1 ULTIMATE TENSILE STRENGTH

Ultimate tensile strength (UTS), often shortened to tensile strength (TS) or ultimate strength is the maximum stress that a material can withstand while being stretched or pulled before failing or breaking. It is usually found by performing a tensile test and recording the stress versus strain the highest point of the stress-strain curve is the UTS. It is an intensive property therefore its value does not depend on the size of the test specimen. However, it is dependent on other factors, such as the preparation of the specimen, the presence or otherwise of surface defects, and the temperature V the test environment and material. Tensile strengths are rarely used in the design of ductile members, but they are important in brittle members. Tensile strength is defined as a stress, which is measured as force per unit area. In the SI system the unit is the pascal (Pa) (or a multiple thereof, often mega pascals (MPa), using the mega - prefix); or, equivalently to pascals, newtons per square meter (N/m²). The customary unit is pound-force per square inch (lbf/in² or psi), or kilo-pounds per square inch (ksi, or sometimes kpsi), which is equal to 11000 psi; kilo-pounds per square inch are commonly used for convenience when measuring tensile strengths.



Figure 2. Universal Tensile Machine

Many materials display linear elastic behavior, defined by a linear stress-strain relationship, as shown in the figure, in which deformations are completely recoverable upon removal of the load; that is, a specimen loaded elastically in tension will elongate, but will return to its original shape and size when unloaded. Beyond this linear region, for ductile materials, such as steel, deformations are plastic. A plastically deformed specimen will not return to its original size and shape when unloaded. There will be elastic recovery of a portion of the deformation. For many applications, plastic deformation is unacceptable, and is used as the design limitation. After the yield point, ductile metals will undergo a period of strain hardening, in which the stress increases again with increasing strain, and they begin to neck, as the cross-sectional area of the specimen decreases due to plastic flow. In a sufficiently ductile material, when necking becomes substantial, it causes a reversal of the engineering stress-strain curve this is because the engineering stress is calculated assuming the original cross-sectional area before necking. The reversal point is the maximum stress on the engineering stress-strain curve, and the engineering stress coordinate of this point is the tensile ultimate strength.

3.2 YIELD STRENGTH

The yield strength or yield point of a material is defined in engineering and materials science as the stress at which a material begins to deform plastically. Prior to the yield point the material will deform elastically and will return to its original shape when the applied stress is removed. Once the yield point is passed, some fraction of the deformation will be permanent and non-reversible. In the three-dimensional space of the principal stresses ($\sigma_1, \sigma_2, \sigma_3$), an infinite number of yield points forms together a yield surface. Knowledge of the yield point is vital when designing a component since it generally represents an upper limit to the load that can be applied. It is also important for the control of many materials production techniques such as, rolling or pressing. In structural engineering, this is a soft failure mode as it does not normally cause catastrophic failure or ultimate failure unless it creates buckling. Typical yield behavior following stresses as seen from figure 3.

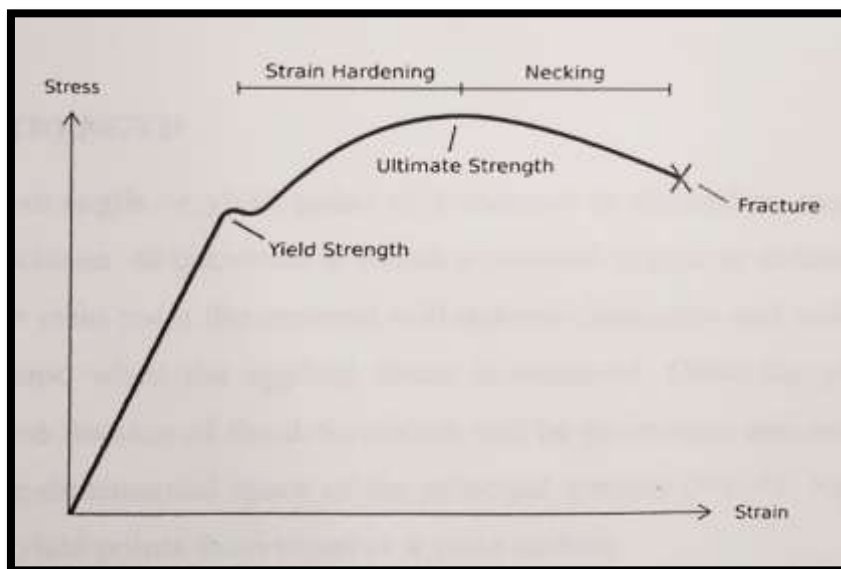


Figure 3: A typical Stress Strain Curve

3.2.1 True Elastic Limit

The lowest stress at which dislocations move. This definition is rarely used, since dislocations move at very low stresses, and detecting such movement is very difficult. Proportionality limit Up to this amount of stress, stress is proportional to strain, so the stress-strain graph is a straight line, and the gradient will be equal to the elastic modulus of the material.

3.2.2 Elastic Limit (Yield Strength)

Beyond the elastic limit, permanent deformation will occur. The lowest stress at which permanent deformation can be measured. This requires a manual load- unload procedure, and the accuracy is critically dependent on equipment and operator skill. For elastomers, such as rubber, the elastic limit is much larger than the proportionality limit. Also, precise strain measurements have shown that plastic strain begins at low stresses.

3.2.3 Yield Point

The point in the stress-strain curve at which the curve levels off and plastic deformation begins to occur.

3.2.4 Offset Yield Point (Proof Stress)

When a yield point is not easily defined. The value for this is commonly set at 0.1 or 0.2% of the strain. The offset value is given as a subscript, e.g. $R_{p0.2} = 310$ MPa. High strength steel and aluminum alloys do not exhibit a yield point, so this offset yield point is used on these materials.

3.2.5 Upper Yield Point And Lower Yield Point

Some metals, such as mild steel, reach an upper yield point before dropping rapidly to a lower yield point. The material response is linear up until the upper yield point, but the lower yield point is used in structural engineering as a conservative value. If a metal is only stressed to the upper yield point, and beyond, Luders bands can develop.

3.3 Hardness

Hardness is a measure of how resistant solid matter is to various kinds of permanent shape changes when a force is applied. Macroscopic hardness is generally characterized by strong intermolecular bonds, but the behavior of solid materials under force is complex; therefore, there are different measurements of hardness: scratch hardness, indentation hardness, and rebound hardness. hardness is dependent on ductility, elastic stiffness, plasticity, strain, strength toughness, and viscosity. Common examples of hard matter are ceramics, concrete, certain metals and superhard materials, which can be contrasted with soft matter. here are three main types of hardness measurements: Scratch, indentation, and bound. Within each of these classes of measurement there are individual measurement scales.

IV. METHODOLOGY

The research work comprised of testing four ferrous specimens of different diameters with different compositions. First phase of research work comprises of testing tensile strength, hardness and elongation. Hardness Tests will be conducted on Universal Testing Machine and Rockwell testing machine.

4.1 Procedure For Testing

The specimen to be tested is placed in the machine between the grips and an extensometer if required can automatically record the change in gauge length during the test. If an extensometer is not fitted, the machine itself can record the displacement between its cross heads on which the specimen is held. However, this method not only records the change in length of the specimen but also all other extending / elastic components of the testing machine and its drive systems including any slipping of the specimen in the grips. Once the machine is started it begins to apply an increasing load on the specimen. Throughout the tests, the control system and its associated software record the load and extension or compression of the specimen. The Rockwell scale is a hardness scale based on the indentation hardness of a material. The Rockwell test determines the hardness by measuring the depth of penetration of an indenter under a large load compared to the penetration made by a preload. There are different scales, denoted by a single letter, that use different loads or indenters. The result is a dimensionless number noted as HRA, where A is the scale letter.



Figure 5. Rockwell Hardness Testing Machine

When testing metals, indentation hardness correlates linearly with tensile strength. This important relation permits economically important nondestructive testing of bulk metal deliveries with lightweight, even portable equipment, such as hand-held Rockwell hardness. Also, testing needs no surface preparation of specimen whose hardness is to be tested.

4.2 Optical Emission Spectrometer

It is an elementary analysis device by optical emission spectrometry on laser produced plasma, the device comprising: a pulsed laser source; a diaphragm having an aperture of a fixed diameter for selecting part of a laser beam emitted by laser source on an object to be analysed, laser beam not being focused in the plane of said diaphragm, first optical means projecting the image of the diaphragm to infinity, second optical means receiving the image of said diaphragm projected to infinity by the first optical means and focusing it on object to be analysed to produce plasma on the surface of the object, wherein the image of said diaphragm focused on said object is equal to a required dimension on the object, said required dimension corresponding to a required spatial resolution; and the focal point of laser beam, after crossing through said diaphragm and first and second optical means, is outside the image plane of the diaphragm. It serves as the means for analyzing a light radiation spectrum by the plasma, as the means for analyzing disposed adjacent to the Plasma, means for determining the elementary composition of said object from means for analyzing a light radiation spectrum; and means for displacing said object within a plane after each pulse of said laser source. Different parts of optical emission spectrometer are shown in Figure 6.



Figure 6 Optical Emission Spectrometer

A greatly reduced inner volume combined with an optimized argon flow reduces the argon consumption in the spark stand by about a factor of two while simultaneously reducing the amount of condensate. A further, drastic decrease in the argon required is possible using the new argon saving module. The spectromaxx automatically begins to flush the spark stand on time for the start of work—for example, the next morning, or at the beginning of the week or after vacation. The window to the optical system can be quickly changed without tools if necessary.

Also it is pertinent to mention that the sample clamp can be swiveled to both sides and has an integrated safety circuit; enabling rapid sample changes. Also, special adapters are available for the analysis of small pieces. The special optic in the spectromaxx is accommodated together with the accompanying components, in a closed housing that effectively protects it from dust. The spectromaxx uses the wavelength range from 140 to 670 nm. The applicable and configured wavelength range is based on the customer's application requirements.

4.3 Spark Analyzer Vision Software

It provides a simple, intuitive interface with numerous functions for the setting of instrument parameters, for data exchange with external computers and for the printing and evaluation of results based on an integrated SQL databank. A comprehensive diagnosis system monitors and continuously documents the satisfactory operational state of the system. Any malfunctions can be localized, identified and displayed in a schematic view of the instrument. The regular measurement of control samples at a pre-set time can be managed using the diagnosis system.

V. EXPERIMENTATION RESULTS

From testing specimens on UTM and Optical Spectrometer following data has been obtained as tabulated in Table 1 and Table 2

Table 1. Data obtained from testing of specimen on UTM and Hardness testing machine

S. No	Specimen content (in %age)	Carbon	Ultimate Strength (in N/mm ²)	Yield Stress (in N/mm ²)	Percentage Elongation (in %age)	Hardness (in HRB)
1	0.18		610	436	0.25	91
2	0.406		667	563	0.5	91.5
3	0.442		727	479	0.76	90
4	1.021		784	655	1.13	101.5
5	2.02		722	499.8	1.28	93.1

Table 2. Data obtained from Spectroscopy Analysis of Specimens

Constituent Elements (in %age) Diameter of Sample (in mm)	C	Si	Mn	Cr	Ni	Mo	Cu	P	S	Fe
20.2	0.442	0.279	0.713	0.062	0.022	0.002	0.045	0.035	0.0358	98.33
20.7	2.021	0.161	0.423	1.042	0.074	0.012	0.009	0.035	0.0204	96.73
21.8	1.021	0.306	0.521	1.101	0.102	0.024	0.178	0.049	0.0484	96.61
22.0	0.406	0.285	0.513	1.294	1.32	0.020	0.010	0.017	0.0157	95.79

The data so obtained is represented graphically

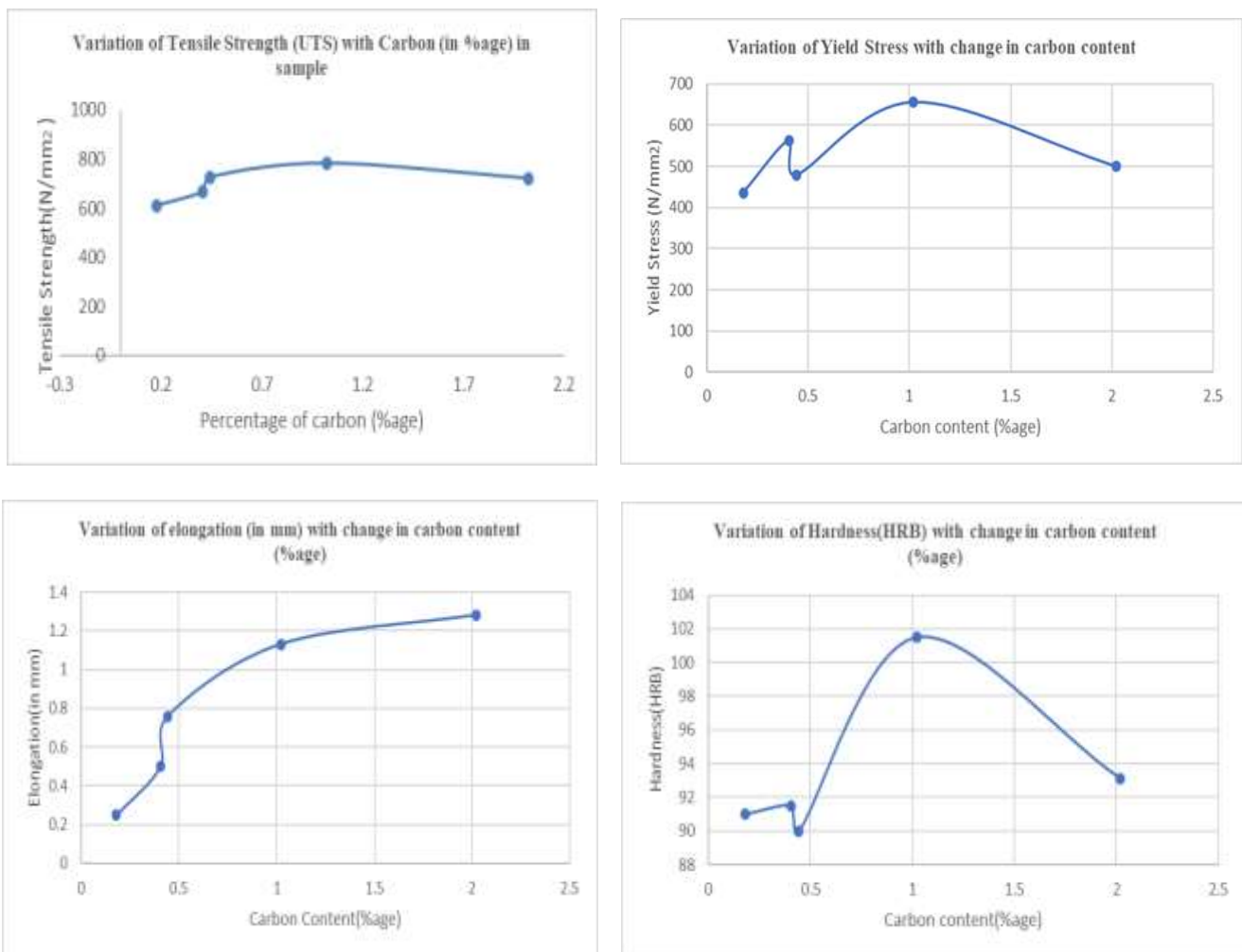


Figure 7. Graphs depicting variation of hardness, tensile strength, yield stress and elongation of specimen with variation in carbon percentage

5.2 Microstructure of the specimens

The specimens were surface cleaned and etched with 2 percent nitrox solution, then etched surface was put under microscope zoomed up to 100X revealed following structure.



Diameter 20.2 mm



Diameter 20.7 mm



Diameter 21.8 mm



Diameter 22.0 mm

Figure 8 Microstructure of Etched Specimen at 100 X

VI. CONCLUSIONS

Based on the results trends, following conclusions can be drawn;

- It seems that the properties of the samples are influenced by the concentrations of certain elements in the samples, particularly carbon, iron, manganese, and silicon.
- Sample A has maximum hardness due to higher concentrations of iron and manganese, and lower concentration of silicon. The strong bonds formed by paramagnetic manganese contribute to stronger linkages and increased hardness.
- Sample D exhibits the maximum ultimate tensile strength, attributed to higher silicon content and lower iron and manganese concentrations. Sample A shows the lowest ultimate tensile strength among the samples.
- Sample A experiences the maximum elongation, potentially due to the low silicon concentration leading to increased ductility. Sample D displays the minimum elongation.
- Sample D demonstrates the highest yield strength, while Sample A shows the lowest yield strength. Presence of silicon, a brittle material, and lower concentrations of iron and manganese in Sample D potentially contribute to the higher yield strength.

VII. FUTURE SCOPE

Microstructural analysis of samples provided insights into the distribution of carbon, silicon, iron, and manganese in the samples. It would be beneficial to understand how the microstructure influences the mechanical properties observed, such as hardness, ultimate tensile strength, elongation, and yield strength.

VIII. ACKNOWLEDGMENT

I am thankful to Mr. Sanjeev Gupta, Head Mechanical Engineering Department, GCET, Jammu for his guidance and allowing me to carry out research work in a time bound manner .

REFERENCES

1. Srijumpan W Wiengmoon A, Morakotjinda M, Krataitong R Yotkaew T, Tosangthum N and Tong Sri R 2015 Mater. Des. 88 693-701
2. Pandit A.S and Bhadeshia HKDS 2012 Proc. R. Soc. A468 2767-2778
3. Lu Z Wang B Wang Z Sun S and Fu W 2013 Mater: Sci. Eng A547 143-148.
4. Smallman RE 2013 Modern Physical Metallurgy (Amsterdam, Netherlands: Elsevier)
5. Bain E C 1939 Functions of the Alloying Elements in Steel (Cleveland, Ohio: ASM)
6. Ochiai I Nishida S and Tashiro H 1993 Wire J. Int 26 50-61
7. Guo K Fang T Wang J Y Wu A Wang Y Z and Jiang J 2014 Mater. Lett. 134 290-294
8. Tosangthum N Morakotjinda M Krataitong R Wila P Yotkaew T Vetayanugul B Boontatim W and Tong Sri R 2018 Mater Today Proceeding vol 5 9351-9358
9. Andersson D I and Lund T 1993 Creative Use of Bearing Steels ASTM International 171-184
10. Lee H Spanos G J Shiflet J and Aaronson H I 1998 Acta. Metal.1 36 1129-1140
11. Taleff E M Syn C Lesuer D and Sherby O 1996 Metall. Mater. Trans. 27A 111-118
12. Howell P.R and Bee J V 1979 Metall. Trans 10A 1213-1222
13. Cheng W and Li Y 2012 Metall. Mater. Trans. 43A 1817-1825
14. Honda K and Saito S 1920 J. Iron Steel Inst 102 261-267
15. Whitley J 1922 J Iron Steel Inst 105 339-357
16. Luzginova N Zhao L and Sietsma J 2008 Metall. Mater. Trans. A39 513-521
17. Verhoeven J and Gibson E 1998 Metall. Mater. Trans. A29 1181-1191
18. Hackenberg RE and Shiflet G 2003 Acta. Mater. 51 2131
19. Wang J and Van Der Zwaag S 2001 Metall. Mater. Trans 32A 1527-1539
20. Martin J W 2007 Encyclopaedias of the Structure of Materials (Amsterdam, Netherlands: Elsevier)
21. Verhoeven J 2000 Metall. Mater. Trans. 31A (10) 2431-2438
22. Aaronson H I and Domian H 1966 Trans. Metall. Soc. AIME 236 781-796
23. Radko K Hans G and Karl H 1991 Mater. Technol. 62 405-441